Diblock polymeric friction modifier (PFM) in the boundary regime: Tribological conditions leading to low friction

Nasrya Kossoko, Frédéric Dubreuil, Benoît Thiébaut, Michel Belin, Clotilde Minfray

Diblock polymeric friction modifier (PFM) in the boundary regime: tribological conditions leading to low friction

Nasrya F. Kossoko[1, 2], Frédéric Dubreuil[1], Benoît Thiébaut[2], Michel Belin[1], Clotilde Minfray[1]

[1] Ecole Centrale de Lyon, Laboratoire de Tribologie et Dynamique des Systèmes, CNRS-UMR 5513, 36 avenue Guy de Collongue, 69130 Ecully, France

[2] Total Marketing & Services, Centre de Recherche de Solaize, Chemin du Canal, BP 22, 69360 Solaize, France

*Corresponding author: clotilde.minfray@ec-lyon.fr

Abstract:

The aim of this paper is to investigate the tribological conditions required to obtain low friction with a diblock PIB-PEG polymer friction modifier (PFM) blended in base oil (PAO4 + 1% wt PFM) under a severe lubrication regime. Two tribological conditions, rolling/sliding and reciprocating pure sliding, were investigated. A very low friction coefficient ($\mu \sim 0.035$) was obtained at a temperature of 100° C whatever the tribometer used. ECR measurements, ToF-SIMS characterizations of wear tracks and AFM analysis suggested the presence of an adsorbed polymer film on the rubbing surfaces. ToF-SIMS characterizations showed that the polymer bonds to the steel substrate through polar functions.

1. Introduction

Reducing energy losses in tribological contacts is a major challenge facing the manufacturers of devices like thermal engines, cutting machines, bearings, etc. The control and reduction of friction in such contacts is clearly needed. Potential new remedies include the development and uses of new materials, especially materials with improved strength and hardness properties, more effective surface treatments, new designs of moving parts, new lubricants and lubricant additives [1]. The work presented here focuses on the last option.

A lubricant is a multi-constituent fluid composed of a base oil and various additives. These additives provide different functions to the oil: the reduction of temperature sensitivity of oil to viscosity, the protection of friction surfaces against wear through the formation of surface films, keeping component surfaces clean and maintaining the oil's properties within acceptable levels [2]. In addition, other additives reduce friction by making surfaces more slippery. The latter are called friction modifier additives. There are several categories of friction modifier additives such as organic ones: OFMs (organic friction modifiers), Polymer Friction Modifiers (PFMs); and inorganic ones like soluble organo-molybdenum additives and dispersed nanoparticles [3,4].

Indeed, organic molecules are interesting because they respond better to current environmental challenges due to their cost, durability and absence of sulfur content. In recent years, interest has focused on PFMs which show enormous potential for reducing friction under boundary lubrication. Polymers used as friction modifiers are commonly used for biological applications but in aqueous solution [5]. For engine oils, polymers were originally used as Viscosity Index Improvers (VII) to increase the viscosity index in engine and transmission oils, and they have shown their ability to reduce friction in various lubrication regimes [3]. Working on commercial VIIs in mineral oil, Smeeth *et al.* [6] used an optical interferometer to show that VIIs containing polar monomers were able to form a boundary film that can persist up to temperatures higher than 120°C. These films result from the adsorption of the polymer on the two rubbing surfaces to give surface layers that have a higher polymer concentration than the bulk solution and thus they are much more viscous. At low speeds, this viscous surface film fills the contact inlet and controls the amount of fluid entrained. However, at higher speeds, when the EHD film thickness formed by the bulk solution is significantly greater than this viscous layer thickness, the adsorbed polymer no longer enhances fluid entrainment.

Further works confirmed the formation of these thick VII boundary films and also showed that they make a significant contribution to friction and wear reduction [7] at temperatures up to at least 140°C [8]. Up to now, most of these research works have focused on functionalized polymethacrylate polymers (f-PAMAs) [9–12]. Fan *et al.* [11] showed that solutions of diblock copolymers based on a PAMA block and appropriately-functionalized polymethacrylate blocks (especially amine-based functions) give enhanced film thickness and greatly reduced friction under low entrainment speed conditions. These polymers form an adsorbed film with a thickness of around 20 nm on each polar surface, increasing the effective viscosity in the contact and resulting in hydrodynamic lift. Randomly distributed copolymers do not show this type of behavior [11]. In addition, other works have also focused on the study of the morphologies of polymethacrylate polymers to improve their performance as PFMs. These works did not lead to very low friction in pure sliding friction test conditions [13,14].

Recently, a new range of diblock PFMs PIB - PEG, different from polymethacrylate blocks, has been shown to be an interesting PFM additive [15]. Indeed, this PFM offers exceptional

benefits in reducing friction in the boundary and mixed lubrication regimes, both in various base oil groups [15] and in formulated engine oil [4].

Considering the whole family of PFMs, their friction behavior is usually investigated using MTM as Stribeck curves that give information for all lubrication regimes. However, they have been subject to very few studies in reciprocating contacts working under boundary lubrication conditions [4,11,16]. Moreover, apart from the study of friction behavior mentioned above, very few studies exist in the literature on the physico-chemical characterization of rubbed surfaces obtained with PFM, although it would be helpful to understand their organization on surfaces under friction and obtain information on their action mechanism. For example, Tohyama *et al.* [13] used both ToF-SIMS and AFM to analyze rubbed surfaces obtained with a PMA type of PFM. However, regarding OFMs, a large number of other characterization techniques were used such as Scanning Force Microscopy (SFM)[17–19], Surface Forces Apparatus (SFA)[20], Quartz Crystal Microbalance (QCM)[21,22], FTIR spectroscopy [23,24], Spectroscopy Ellipsometry [22], and so forth.

The objective of this paper is to investigate the tribological conditions required to obtain low friction with the diblock PIB-PEG polymer friction modifier (PFM) blended in a base oil under severe lubrication conditions. To do so, two different tribometers, MTM and a reciprocating ball-on-flat tribometer, are used. Using ToF-SIMS characterizations and AFM analysis, possible friction reduction mechanisms using this PFM in steel / steel contacts are discussed.

2. Materials and methods

2.1. Samples

The Polymer Friction Modifier (PFM) additive known as Perfad 3050 (Croda Lubricants) is a patented diblock PIB-PEG copolymer with an average molar mass expected from the patent to be around 3500 g/mol [15]. The average molar mass of the PIB part is 1000 g/mol and the molar mass of the PEG part is 600 g/mol. The chemistry used for the linkage between the PIB and PEG parts lead to the formation of multi-ester bonds [15]. The poly-α-olefin base oil (PAO 4) with kinematic viscosities η (100°C) = 4 mm^2/s and η (40°C) = 17.5 mm^2/s was provided by Total. The typical lubricant used in this paper is composed of 1% wt of PFM blended in PAO 4 base oil and stirred at 60°C for 2 hours.
An MoDTC-based lubricant (PAO 4 + 1% wt MoDTC), prepared as described above, was used for comparison as MoDTC is a well-known friction modifier. The MoDTC additive was provided by Total.

All the tribological tests used hardened AISI 52100 steel with a Young's modulus of 210 GPa. The samples used for the MTM tests (balls and discs) were bought from PCS Instruments (Rq_{Ball} = 20 nm, Rq_{Disc} = 2 nm). Balls with a radius of 9.5 mm were employed. For the reciprocating tribometer tests, balls (2.25 mm radius) and flats were purchased from CIMAP and PCS Instruments, respectively (Rq_{Ball} = 25 nm, Rq_{Flat} = 2 nm).

2.2. Tribological tests

Two different tribometers were used: MTM and reciprocating ball-on-flat. Specimens were cleaned before the friction test by ultrasound in acetone, heptane and isopropanol successively; 15 mins in each solvent.

2.2.1. MTM test

A Mini Traction Machine (MTM) from PCS Instruments was used to evaluate the frictional properties of the lubricant.
Stribeck curves are usually plotted for MTM under rolling - sliding conditions. The parameter SRR (Slide-to-Roll Ratio) is defined as the ratio of the sliding speed $|U_B - U_F|$ to the entrainment speed ($U = (U_B + U_F)/2$) where U_B and U_F correspond to ball and disc speeds, respectively. The SRR is given by the following formula: $SRR = |U_B - U_F|/U$ [25].
The MTM test procedure consisted of performing three different steps: an initial Stribeck curve (step 1), then 60 min rubbing (step 2), and a final Stribeck curve (step 3). The temperature, SRR and rubbing speed of the rubbing step (step 2) were varied to evaluate their impacts on the friction behavior.
All the Stribeck curves were plotted over the entrainment speed range of 2200 mm/s (at least) to 3 mm/s (tests carried out at SRR 50% can start at 2500 mm/s). They were obtained by decreasing the entrainment speed while maintaining a fixed Slide-to-Roll Ratio SRR from higher to lower speed in order to switch from a full-film lubrication regime to a more severe lubrication regime. The load applied was 40 N, corresponding to a maximum Hertz pressure of 1 GPa. The contact between the disc and the ball was completely immersed in the lubricant oil. The test was performed twice for each test condition studied.

MTM Friction parameter	
Lubricant	PAO4 + 1% wt P3050
Temperature	25°C, 100°C
Load/ Pmax Hertz	40 N/ 1 GPa
SRR	50%, 100%, 150%
Entrainment speed (Steps 1 and 3)	2200 – 3 mm/s
Rubbing speed (Step 2)	3, 10, 50, 100 mm/s

Table 1: Experimental conditions used during MTM friction tests

2.2.2. Reciprocating tribometer test

A home-made reciprocating ball-on-flat tribometer was used to perform tribological tests under boundary conditions. The friction behavior of PFM was studied by performing tests with varying parameters such as sliding speed, normal load and temperature (cf. Table 2). A few drops of oil were used for each test (100 µL). All the tests were run for 1000 cycles with a stroke length of 3 mm. A "steady state" was generally achieved between 500 and 1000 cycles. The average steady state friction coefficient of each test was calculated taking into account the friction values from the last 500 cycles. The tests were repeated at least 6 times per condition.

The electrical contact resistance (ECR) was also measured throughout the friction test for the specific test [19]. A low voltage of about 7 mV was applied between the ball and the flat. The resulting current was measured using a logarithmic current amplifier to cover a wide range of resistance from 1 to 10^7 Ohm.

Reciprocating Tribometer Friction parameter	
Lubricant	PAO4 + 1% wt PFM
Temperature	25°C, 100°C
Load /Pmax Hertz	0.5 N /0.6 GPa 2 N /1 GPa 5 N /1.4 GPa
Speed	1 mm/s 3 mm/s 10 mm/s
Stroke length	3 mm
Cycles	1000

Table 2: Experimental conditions used during reciprocating friction tests.

Lubricant film thicknesses and lambda ratio were evaluated for step 2 of MTM tests and for reciprocating tests. The results are reported in SM1.

2.3. ToF-SIMS analysis

Time of Flight - Secondary Ion Mass Spectometry (ToF-SIMS) analyses were performed on ToF-SIMS 5 ION-TOF. Negative ion depth profiles were obtained inside and outside the friction scars after the different friction tests. A low-energy Cesium gun (500 eV – 20nA), rastered on 350 x 350 µm², was used to etch the sample during depth profiling and a Bismuth gun (25 keV – Bi_3^+ - 0.25pA) was used for ToF-SIMS analyses.

ToF-SIMS is a surface sensitive technique (depth analyzed, around 1 nm) with high resolution in mass (femtomole) and with a detection threshold from a few ppb to a few hundred ppm depending on the elements. The area analyzed was 100 x 100 µm².

The samples were tilted and the oil was drained through tissue paper after all the friction tests and before ToF-SIMS analyses. The excess oil was removed by capillary transfer with an aluminum foil.

After the ToF-SIMS profiles were acquired, several of the elements detected were quantified. The areas "A" under the Tof-SIMS profile curves were estimated, taking into account a baseline and using "Origin" software for integration.

2.4. AFM analysis

AFM measurements were carried out with a Pico Plus (Molecular Imaging) equipped with silicon probes having a nominal spring constant of 37 $N.m^{-1}$ and a nominal tip radius of 6 nm (ACTA AFM probes from App nano), using a dedicated standard liquid cell and a heater for *in situ* measurement at 100°C. Data were treated and analyzed using Gwyddion free software.

"Nanoshaving" measurements were performed to show whether the additive was adsorbed on the surface of the steel flat or not. First, imaging local areas (2x2 μm^2) in contact mode with a high force set point (1-2 mN) was performed to remove any material that could be adsorbed at the surface. Then, further imaging of larger areas (10x10 μm^2) in tapping mode was carried out to visualize the "nanoshaved" area.

2.5. Dynamic Light Scattering (DLS)

DLS data were recorded on a Nanosizer nano-S (Malvern, Ltd, UK) with a lubricant composed of 1% wt of PFM blended in PAO 4 base oil. A dedicated quartz cell with a 1 cm path length was filled with 30 µL of sample to perform the measurement.

The data collected from this experiment were hydrodynamic radii. DLS measurements were performed over a temperature range from 20°C to 90°C by making an acquisition every 10°C. The results are shown in supplementary materials SM2.

3. Results and discussion

In this part, the results of the friction tests and the characterizations of rubbed samples are shown. The lubricant, PAO4 + 1% wt PFM, and the base oil, PAO4, were both tested with the MTM and the reciprocating ball-on-flat tribometer. A Mo-based lubricant PAO4 + 1% wt MoDTC was used to make comparisons between tests at 100°C only.

3.1. MTM test

The effect of temperature on the friction behavior of the PFM was first investigated on the MTM tribometer. The friction reduction capabilities of the PFM at 100°C were then compared to the classical MoDTC friction modifier under the same contact conditions. The effect on the friction behavior of the PFM of the rubbing speed and the SRR were then studied.

3.1.1 Effect of temperature

The MTM test procedure was divided into three steps: an initial Stribeck curve (step 1), then 60 mins of rubbing (step 2) and a final Stribeck curve (step 3). The tests were carried out at SRR = 50%, a contact pressure of 1 GPa and the rubbing step was performed at 100 mm/s rubbing speed. The first Stribeck curves are represented by solid lines and the last Stribeck curves are plotted with dotted lines. Two different temperatures were tested: 25°C (blue curves) and 100°C (orange curves).

The friction tests results are shown in Figures 1 and 2. They represent, respectively, comparative friction tests between base oil PAO 4 and PAO 4 + 1% wt PFM at 25°C and 100°C on the one hand and comparative friction tests between PAO 4 + 1% wt PFM and PAO 4 + 1% wt MoDTC at 100°C only, on the second hand. In Figures 1 and 2, column (a) shows the two Stribeck curves (steps 1 and 3). Column (b) shows the histograms of the averaged friction coefficient obtained on the Stribeck curves over low entrainment speeds from 3 to 10 mm/s (severe test conditions). Column (c) shows the 60 mins rubbing curves (step 2).

Stribeck curves (Steps 1 and 3)

As can be seen in Figure 1 (a), the initial and final Stribeck curves (solid line and dotted line) are closely superimposed at both temperatures for base oil PAO 4 and PAO 4 + 1% wt PFM. Since these two curves are practically the same, this suggests that for lubricant PAO 4 + 1% wt PFM, the polymer film may increase inside the contact before the 60 mins rubbing (step 2) and it is not modified further during step 2.

Figure 1 (a) also shows that, towards low speeds, all the PAO 4 Stribeck curves at 25°C and 100°C almost converge to the same friction coefficient values near 0.1. This is illustrated in figure 1 (b) by the average of the friction coefficients calculated from 10 mm/s to 3 mm/s for Stribeck curves (step 1 or 3). At 25°C, the friction coefficients of the first and last Stribeck curves are evaluated at 0.099 ± 0.007 and 0.105 ± 0.009, respectively. At high temperature 100°C, they are estimated at 0.111 ± 0.006 and 0.106 ± 0.003, respectively.

However, in the presence of the PFM, the friction levels are lower, especially at 100 ° C (Figure 1 (a)). At 25°C , the average friction coefficient at low speeds from 10 mm/s to 3 mm/s (figure 1 (b)) was evaluated at 0.075 ± 0.008 for the first Stribeck curve (step 1) and at 0.072 ± 0.008 for the last Stribeck curve (step 3). At 100°C, they were evaluated at 0.025 ±

0.003 for the first Stribeck curve (step 1) and at 0.023 ± 0.004 for the last Stribeck curve (step 3).

Rubbing curves (Step 2)

Concerning the rubbing curve in figure 1 (c), the rubbing curves are very stable for all the tests. For the base oil PAO 4, the average values of friction coefficients are estimated at 0.049 ± 0.001 (25°C) and at 0.064 ± 0.001 (100°C). The friction levels are the lowest at 25°C. Which is consistent with the viscosity of the oil. Since the oil becomes more viscous as the temperature decreases, the oil film thickness in the contact was thicker at 25°C than at 100°C.

In the presence of additive, we noted the opposite effect. The average values of friction coefficients are estimated at 0.049 ± 0.001 (25°C) and at 0.033 ± 0.001 (100°C). The friction levels are the lowest at 100 °C. This is surely due to the action of this additive in the contact. When the oil film becomes very thin, the friction in the contact was controlled by the polymer film formed on the contact surface.

Thus, knowing that the polymer was indeed active at 100°C, the rest of the MTM tests were carried out at this temperature.

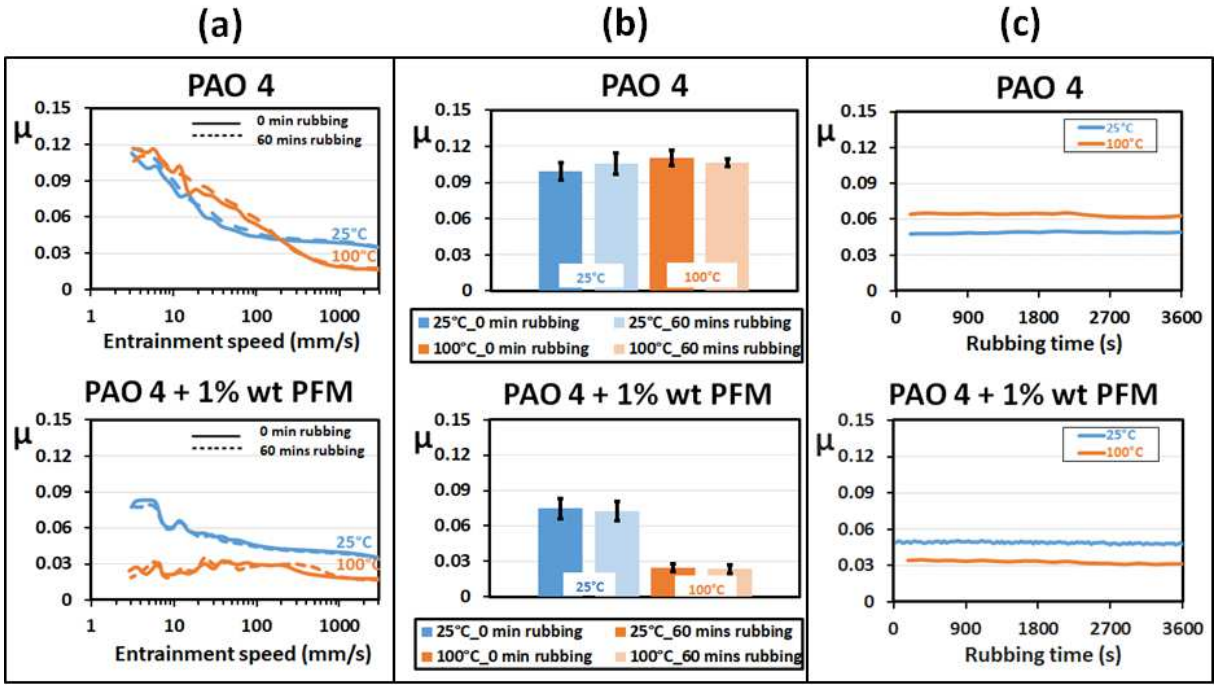

Figure 1: Comparative MTM friction tests between Base oil PAO 4 and PFM-based lubricant (PAO 4 + 1% wt PFM). In (a) Stribeck curves of the MTM tests at 25 °C (blue) and at 100 °C (orange) at SRR = 50%. In (b) histograms of the coefficients of friction values averaged over low speeds between 3 and 10 mm/s. In (c) rubbing curves between Stribeck curves at SRR = 50%, 100 mm/s.

3.1.2 Comparison of PFM friction behavior at 100°C to classical MoDTC friction modifier

MoDTC is a well-known friction modifier currently used in industrial lubricants. The friction behavior of the PFM (PAO 4 + 1% wt PFM) was compared to MoDTC ones (PAO 4 + 1% wt MoDTC) under the same contact conditions to compare their abilities to reduce friction at 100°C.

Stribeck curves (Steps 1 and 3)

Figure 2 (a) shows that for PAO 4 + 1% wt PFM and PAO 4 + 1% wt MoDTC, the initial and final Stribeck curves (solid line and dotted line) closely overlap and that very low friction is obtained at 100°C.
Regarding Figure 2 (b), the average friction coefficient values at low speeds from 10 mm/s to 3 mm/s for the PFM-based lubricant are estimated at 0.025 ± 0.003 (first Stribeck curve - step 1) and at 0.023 ± 0.004 (last Stribeck curve - step 3). Concerning the MoDTC-based lubricant, they are evaluated at 0.050 ± 0.002 (step 1) and at 0.054 ± 0.002 (step 3).

Rubbing curves (Step 2)
As shown in Figure 2 (c), the rubbing curves corresponding to the two lubricants are both very stable over the 60 min rubbing period.
The average friction coefficient values are estimated at 0.033 ± 0.001 for the PFM-based lubricant and at 0.043 ± 0.001 for PAO 4 + 1% wt MoDTC.

The comparative study of friction at 100°C performed between the two additives, the PFM studied and the MoDTC Friction Modifier, show that all the friction tests performed at 100°C (Stribeck curves and Rubbing curves) lead to very low friction, even for the most severe conditions. The aim of comparing MoDTC and PFM was to show that for low sliding speeds, and such severe lubrication conditions, the same range of low friction coefficients can be obtained with this PFM and with a well-established boundary friction modifier like MoDTC.

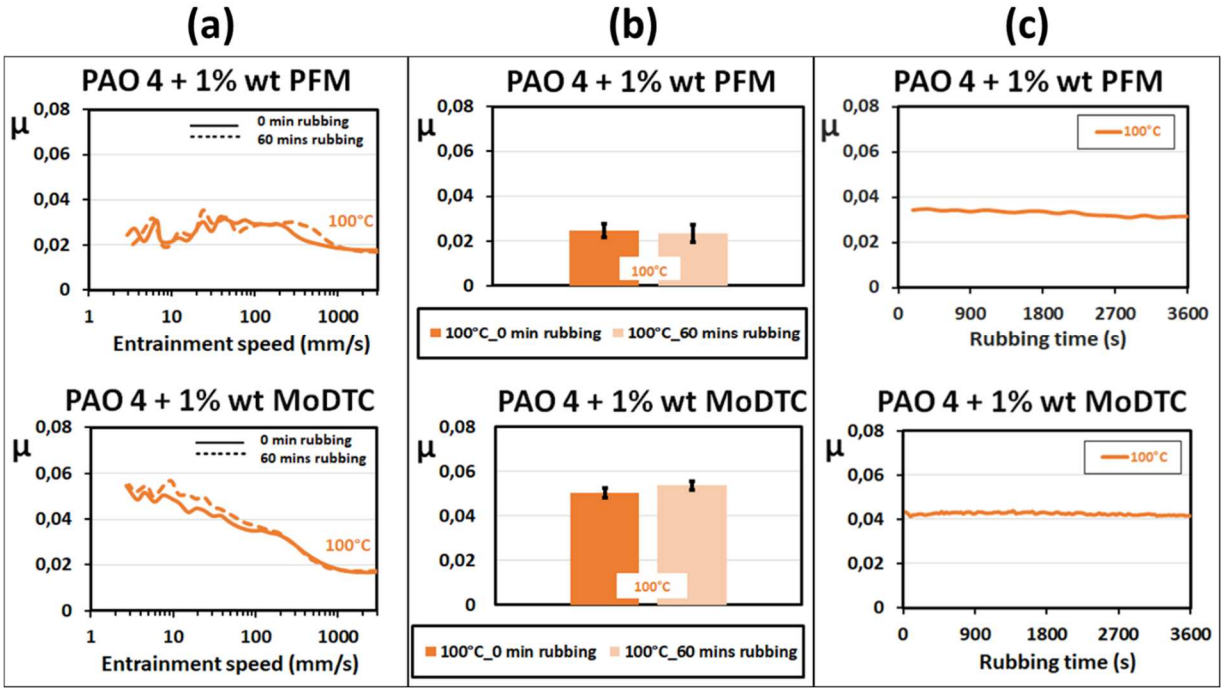

Figure 2: Comparative MTM friction tests between PFM-based lubricant (PAO 4 + 1% wt PFM) and MoDTC-based lubricant (PAO 4 + 1% wt MoDTC). In (a) Stribeck curves of the MTM tests at 100 ° C (orange) at SRR = 50 %. In (b) histograms of the coefficients of friction values averaged over low speeds between 3 and 10 m/s. In (c) rubbing curves between Stribeck curves at SRR = 50%, 100 mm/s.

3.1.3 Effect of rubbing speed (step 2)

In an MTM test, there is a 60 min rubbing step (step 2) between the first and last Stribeck curves (step 1 and 3). Four different rubbing speeds are tested: 100 mm/s, 50 mm/s, 10 mm/s and 3 mm/s at these conditions: 100°C, 1 GPa and 50% SRR. They are represented in blue, yellow, red and black, respectively (Figure 3). Lower speeds allow for more severe test conditions. This rubbing step 2 was also thought to lead to the accumulation of additive in the contact to form a thick film. If this hypothesis is true, we should notice a decrease in the friction coefficient on the last Stribeck curve compared to the first one.

Stribeck curves (Steps 1 and 3)

The first and last Stribeck curves are plotted in Figure 3 (a). The first Stribeck curves are drawn with solid lines and the last Stribeck curves with dotted lines. Figure 3 (b) shows the histograms of averaged friction coefficients over low speeds from 3 to 10 mm/s (severe test conditions). To facilitate identification, we have represented the results of the first Stribeck curves in dark colors and those of the last Stribeck curves in light colors. Figure 3 (c) presents the 60 mins rubbing curves.

By comparing all the Stribeck curves (initial and final) for these four different rubbing speeds tested, we noticed that they are all almost superimposed and converge to low friction ≈ 0.05 at low entrainment speeds (Figure 3 (a)). In (b), the average values of the friction coefficients calculated from the Stribeck curves between 10 mm/s to 3 mm/s also show these low friction coefficients whatever the rubbing speed at step 2. For each rubbing speed, the following values are the average friction coefficients for the initial and final Stribeck curves, respectively. At 100 mm/s, $\mu = 0.049 \pm 0.002$ and 0.043 ± 0.002; at 50 mm/s, $\mu = 0.052 \pm 0.003$ and 0.047 ± 0.002; at 10 mm/s, $\mu = 0.046 \pm 0.002$ and 0.058 ± 0.002; at 3 mm/s, $\mu = 0.047 \pm 0.004$ and 0.052 ± 0.003.

Rubbing curves (Step 2)

The different rubbing curves (step 2) presented in figure (c) also display low friction coefficients. The average values of the friction coefficients are estimated as follows: $\mu = 0.037 \pm 0.001$ (Rubbing speed = 100 mm/s), $\mu = 0.043 \pm 0.003$ (Rubbing speed = 50 mm/s), $\mu = 0.052 \pm 0.002$ (Rubbing speed = 10 mm/s) and $\mu = 0.040 \pm 0.003$ (Rubbing speed = 3 mm/s).

Overall, the variations of rubbing speeds at step 2 from 3 mm/s to 100 mm/s do not seem to have a marked effect on friction levels.

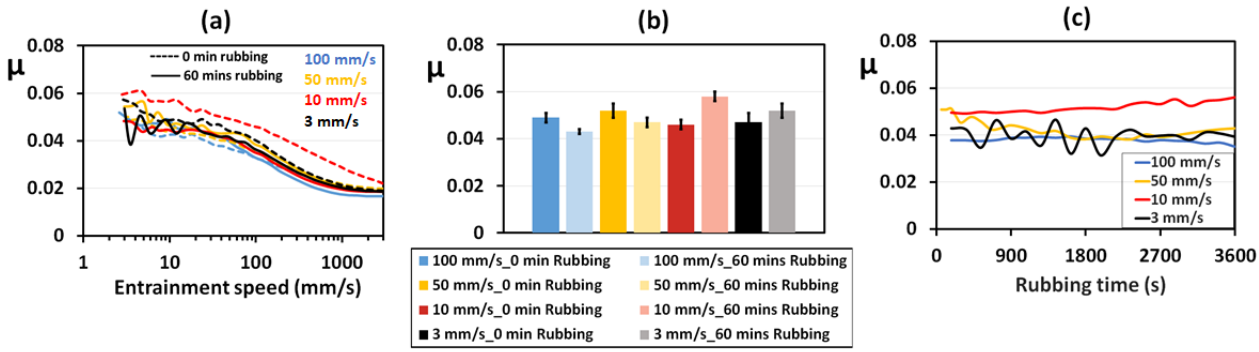

Figure 3: In (a) the Stribeck curves of the MTM tests at 100 ° C as a function of rubbing speed for the lubricant (PAO 4 + 1% wt PFM). In (b) the histograms of the averaged coefficients of friction calculated over low speeds between 3 and 10 mm/s from the Stribeck curves. The friction coefficients measured during rubbing step 2 between the Stribeck curves are shown in (c)

3.1.3 Effect of SRR

Three different SRRs (50%, 100% and 150%) were performed and the test results are represented in red, green and purple, respectively (Figure 4). Tests were carried out at 100°C and at a contact pressure of 1 GPa. Rubbing step 2 was performed at 10 mm/s.

Stribeck curves (Steps 1 and 3)

Figure 4 (a) shows the first and last Stribeck curves plotted in solid line and dotted line respectively for each test condition (steps 1 and 3). Figure 4 (b) presents the histograms of the average friction coefficients calculated from the Stribeck curves over low speeds from 3 to 10 mm/s (first and last curves are drawn in dark and light colors respectively). Figure 4 (c) presents the friction coefficient curves of the 60 min of rubbing during step 2.

By comparing the test friction coefficients for these three SRR values, we note that the Stribeck curves are almost superimposed and converge to a low friction value ≈ 0.05 at low entrainment speeds (Figure 4 (a)).

In Figure 4 (b), the histograms of the average values of the friction coefficients confirm this trend For the first and last Stribeck curves, these values are as follows: $\mu = 0.046 \pm 0.002$ and 0.058 ± 0.002 for test at SRR = 50%, $\mu = 0.050 \pm 0.002$ and 0.058 ± 0.004 for test at SRR = 100%,and $\mu = 0.045 \pm 0.002$ and 0.042 ± 0.002 for test at SRR = 150%.

Rubbing curves (Step 2)

The three different rubbing curves (Figure 4 (c)) also show the same trend for the friction coefficient values of step 2 as the Stribeck curves (step 1 and 3). For this step, the average values of the friction coefficients are estimated at 0.052 ± 0.002 (friction test at SRR = 50%), 0.056 ± 0.002 (friction test at SRR = 100%) and 0.062 ± 0.003 (friction test at SRR = 150%).

Finally, it can be concluded that the variation of SRR from 50% to 150% does not greatly affect the friction coefficient levels.

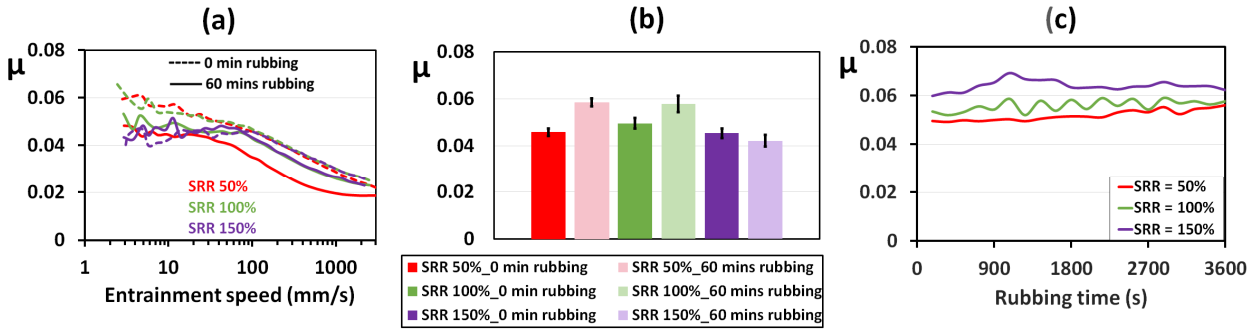

Figure 4: In (a) the Stribeck curves of the MTM tests at 100 °C as a function of SRR for the lubricant (PAO 4 + 1% wt PFM). In (b) the histograms of the friction coefficients averaged over low speeds between 3 and 10 mm/s. The rubbing curves between Stribeck curves in (c).

To conclude on the tests carried out on MTM, although the SRR and the sliding speed did not significantly influence the level of friction, temperature was found to play a significant role. Indeed, low friction coefficients were found at 100°C with PFM compared to 25°C. The results showed acceptable repeatability regarding the standard deviations obtained.

3.2. Reciprocating tribometer test

Figure 5 shows the results of friction tests on a reciprocating ball-on-flat tribometer. Experimental parameters such as pressure, speed and temperature were varied (cf. conditions §2.2.2). These histograms represent the average friction coefficients at steady state obtained for friction tests at the different sliding speeds studied (1 mm/s, 3 mm/s and 10 mm/s). For each sliding speed, three different pressures (0.6 GPa, 1 GPa and 1.4 GPa) and two temperatures (25°C and 100°C) were applied. The blue color indicates the tests performed at 25°C and the orange color represents the tests at 100°C.

There was a marked effect of temperature on the friction levels. In general, at 25°C, the friction coefficient was higher ($\mu \geq 0.07$) than at 100°C ($\mu \leq 0.07$). The lowest friction coefficient $\mu \leq 0.05$ was reached at 100°C both at 0.6 GPa and 1 GPa for all sliding friction speeds.

The very large error bars (+/- standard deviation) at 100°C highlight a significant dispersion of friction coefficient. This could be analyzed considering the presence of two different friction behaviors for the same conditions. This is shown in Figure 6, with the test condition of 3 mm/s, 100°C and 1 GPa. Of the 12 friction curves, some of them present a “high” average steady state friction coefficient (μ around 0.08 plotted in dark blue) and some others, a low friction coefficient (μ around 0.05 presented in light blue). By retracing the histogram as a function of the two different populations, the standard deviation for each population on the friction coefficients is drastically reduced (Cf. figure 5).

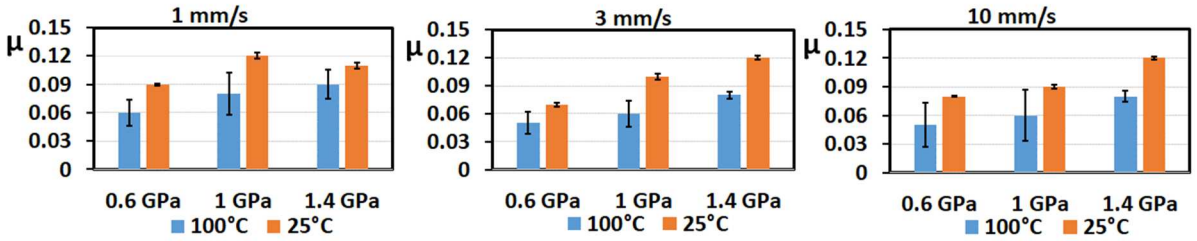

Figure 5: The histograms of the friction results on the reciprocating tribometer for the three friction speeds tested (1mm/s, 3mm/s and 10 mm/s) for the lubricant (PAO 4 + 1% wt PFM). On each graph are the values of the friction coefficient at the different temperatures (25°C and 100°C) and contact pressures (0.6 GPa, 1GPa and 1.4 GPa).

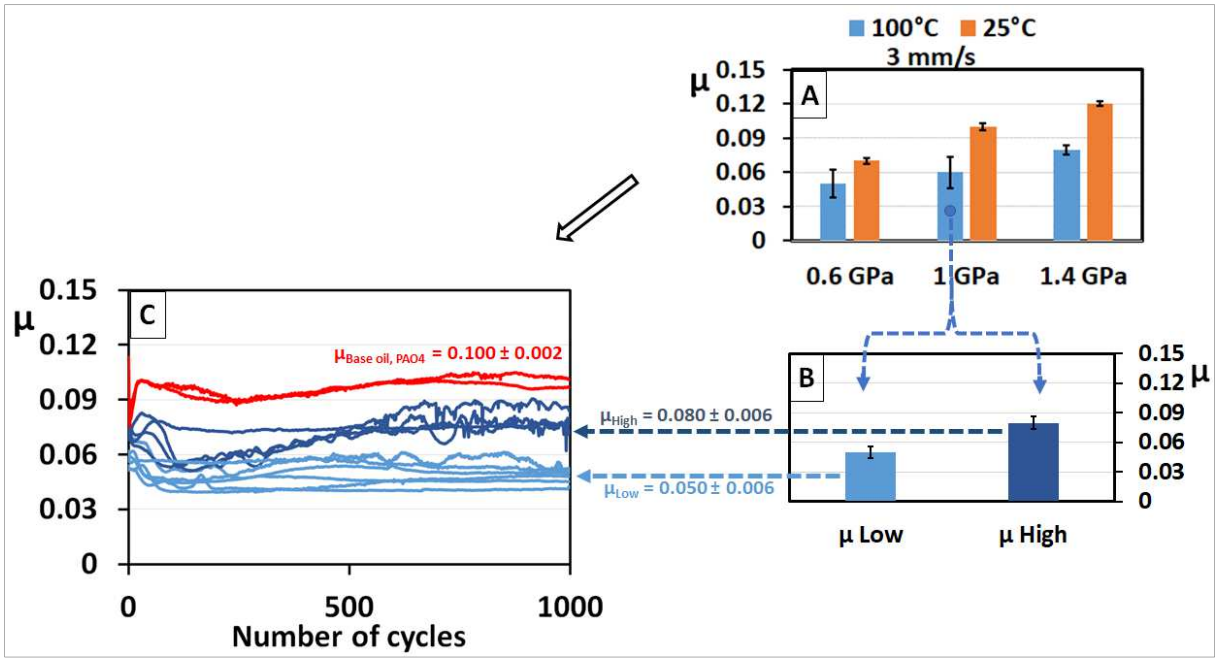

Figure 6: In A the histograms of the friction results on the reciprocating tribometer at 3 mm/s as described in figure 5. In B, the test conditions (3mm / s, 1GPa and 100 ° C) are transformedas a function of friction level into 2 different histograms. In C, friction curves of PAO 4 in red and corresponding friction curves.

3.2.1. Electrical contact resistance measurements

The electrical contact resistance (ECR) was measured simultaneously with the friction coefficient on the reciprocating tribometer for several tests carried out at 100°C, 1 GPa and 3 mm/s. Figure 7 presents the evolution of both the friction coefficient and ECR as a function of the number of cycles.

When the friction coefficient is low (μ = 0.05), the ECR value is very high and vice versa (illustrations with arrows in Figure 7). The ECR measurement indicates there is an insulating layer which separates the opposing rubbing substrate in the contact. This layer is reduced when the friction is high. Thus, it seems that the difference of friction behavior observed is related to a difference of PFM adsorption and/or supply in the interface, which suggests that this polymer interfacial layer is fragile. Furthermore, triboscopic images show that the friction coefficient was constant during the sliding of the ball.

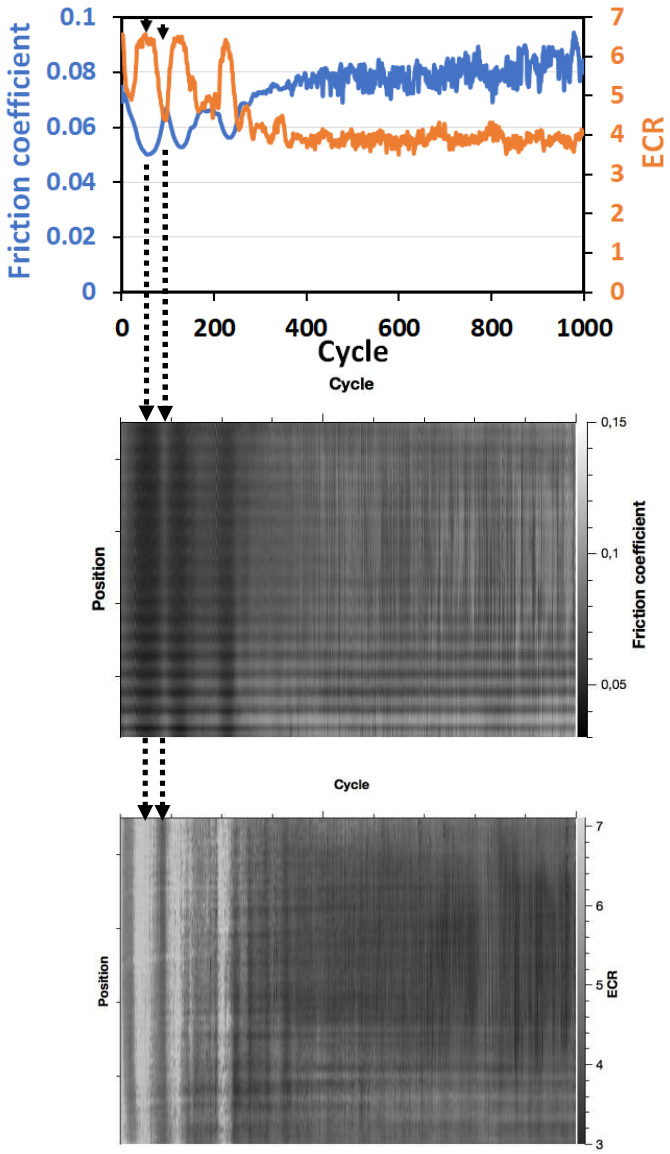

Figure 7: Analysis of both the Friction Coefficient and Electrical Contact Resistance (ECR) curves during the reciprocating test and associated triboscopic images (lubricant PAO 4 + 1% wt PFM).

To summarize, regarding the results obtained for the tests on the reciprocating tribometer, the temperature was also found to be a very important factor for reaching low friction, as with the case for the MTM tests. The lowest friction coefficient was reached ($\mu \leq 0.05$) at 100°C, but at this temperature we noticed a wide dispersion on the friction coefficient which could be analyzed using the two populations of friction coefficients obtained per test conditions: some friction coefficient were high ($\mu \sim 0.08$) while others were low ($\mu \sim 0.05$).

The measurement of ECR together with the friction coefficient showed that an insulating layer of additive was formed in the contact and allowed reaching low friction when it was

well formed. This layer appeared fragile and could explain why the friction reduction capabilities were sometimes lost.

3.3. Tof-SIMS analysis of PFM tribofilm

After different friction tests using the MTM and the reciprocating tribometer, the samples were analyzed by Tof-SIMS profiling inside and outside the friction tracks. The MTM test was carried out at 100°C, 1 GPa and SRR = 50% (steps 1 and 3, lubricant: PAO 4 + 1% wt PFM). The rubbing speed was 100 mm/s at step 2. For the reciprocating tribometer, the test conditions were: 100°C, 1 GPa and 3 mm/s. The samples analyzed were chosen from the friction tests that showed very low friction. The friction coefficient was $\mu = 0.040 \pm 0.001$ for the reciprocating tribometer test and $\mu = 0.040 \pm 0.002$ for the MTM friction test (μ calculated between 10 mm/s to 3 mm/s).

3.3.1. Profiles Tof-SIMS in and out of friction tracks

Abrasion negative ion profiles were performed inside and outside the flat wear tracks after the friction tests (Figure 8)

$C_2H_3O^-$ and $C_3H_3O_2^-$ fragments of molecules could come from the PEG side of the PFM. The other oxygenated species CHO_2^- could belong to an ester function. They could come from the linker part between the PIB and PEG parts of the polymer, as the patent suggests the presence of several ester groups per molecule in this linker [15]. The other species found were C_8H^- (referred to as base oil or PIB polymer part) and $Fe^-/Fe_2O_3^-$ which corresponded to the substrate.

The Tof-SIMS profiles acquired inside and outside all the friction tracks (both MTM and reciprocating tribometer flats) were obtained in the same conditions (Figure 8). They showed the same organization as the polymer film. From the surface to the substrate, we observed in this order: Base oil, Polymer PIB, Polymer PEG/Ester, iron oxide and iron.

For both samples obtained after the MTM and reciprocating tests (disc and flat), the inner and outer Tof-SIMS profiles showed that the CHO_2^- species were found closer to the iron oxide layer followed by the other oxygenated species $C_2H_3O^-$ and $C_3H_3O_2^-$. This is shown in the graphs in Figure 8 using numbers 1 (for the species closest to the substrate), 2 or 3 with each number marked in the color of the species it designates. The results indicate that the oxygen species characteristic of the PFM linker part (CHO_2^-) and the PEG part ($C_2H_3O^-$ and $C_3H_3O_2^-$) were the closest to the iron oxide layer of the substrate. The polymer was probably bonded to the substrate through ester and PEG species.

In case of the reciprocating friction test, the ToF-SIMS profiles were very similar inside and outside the wear scar. This was not surprising, as the amount of wear was very small (cf. optical images in supplementary materials, figure SM3 a)).

It is also interesting to note that the signal of the oxygenated species remained for much longer sputtering time inside the wear track in the case of the MTM experiments compared to the reciprocating tests. This suggests the presence of a thicker adsorbed film. This was confirmed by optical observations, as the wear tracks can be clearly distinguished in the case of MTM test which is not the case for the reciprocating experiment (see Figure in supplementary materials SM3).

Legend of molecules profiles

C_8H^- CHO_2^- $C_2H_3O^-$ $C_3H_3O_2^-$ $Fe_2O_3^-$ Fe^-

Outside wear tracks ***Inside wear tracks***

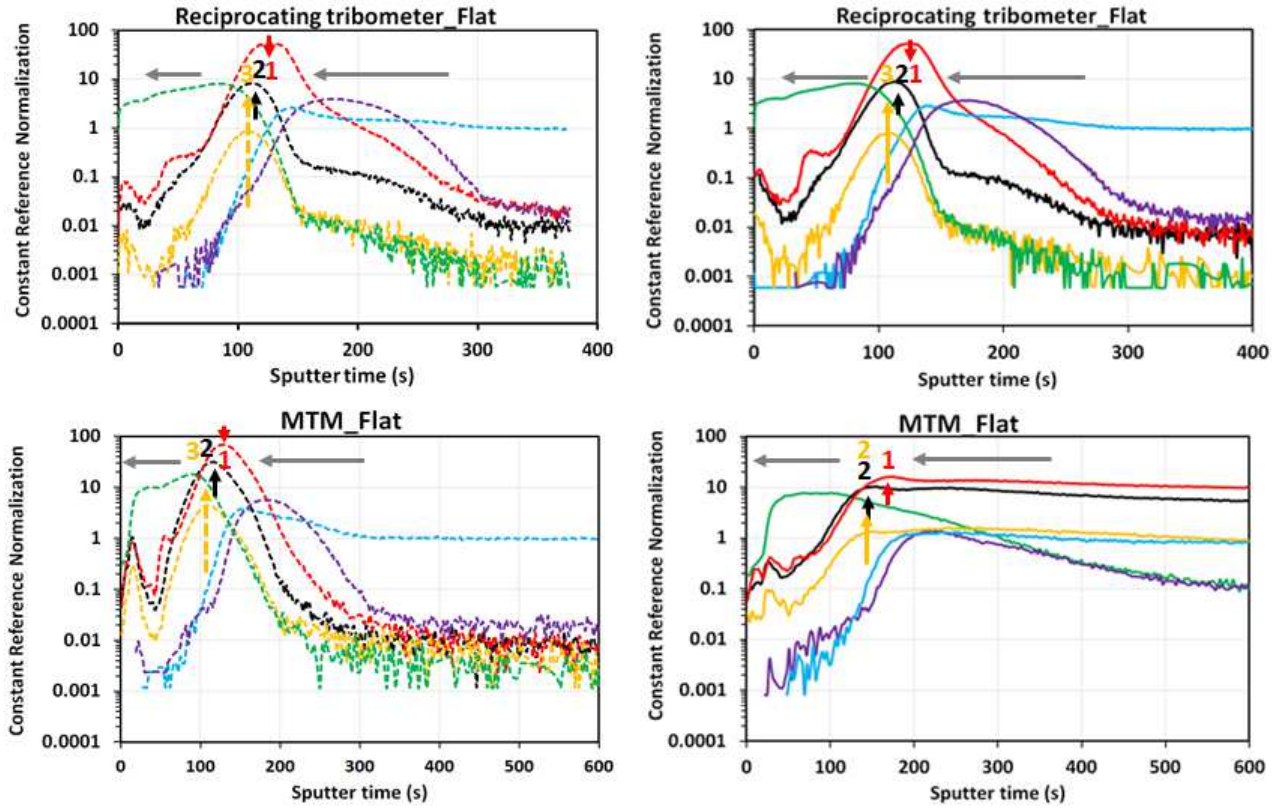

Figure 8: On left, Tof-SIMS profiles obtained outside the flat friction tracks (dotted line) and on right, Tof-SIMS profiles obtained inside the flat friction tracks in solid lines for MTM and reciprocating friction test specimens.

Other additional analyses were carried out on the bare steel following the same cleaning protocol before testing (Figure supplementary material SM4). These Tof-SIMS profiles were obtained in order to check whether the elements identified were not initially present on the steel before the tests.

3.3.2. Profiles Tof-SIMS on cleaned reciprocating tribometer flats

Abrasion negative ion profiles were obtained from a reciprocating tribometer flat after cleaning. The same molecules were detected as observed previously for the Tof-SIMS profiles after friction tests: $C_2H_3O^-$, $C_3H_3O_2^-$, CHO_2^-, C_8H^- and Fe^-, $Fe_2O_3^-$.

Then, we decided to measure and compare the profiles of these elements through the quantification of the areas "A" under the Tof-SIMS profiles curves (cf § for calculation details).
Since iron oxide was an invariable element of the substrate, we therefore evaluated each fragment in relation to $Fe_2O_3^-$. Thus, the ratios of the areas under the curves of ions different from those of the $Fe_2O_3^-$ were then compared between different samples (flat cleaned without friction test and flat after friction test inside and outside the friction tracks).
The comparisons of the ratios were carried out for several fragments characteristic of the PFM molecule: $C_2H_3O^-$, $C_3H_3O_2^-$, CHO_2^-. These results are given in table 4. It is shown that these ions on the cleaned steel flats are much less intense in comparison to those after friction tests inside and outside the friction tracks.
To quantify these differences, we estimated all these values by taking the cleaned steel flat as reference. The $CHO_2^-/Fe_2O_3^-$ ratio was 28.8 times higher inside the friction track compared to the cleaned steel surface. The $C_2H_3O^-/Fe_2O_3^-$ was 126.7 times higher inside the friction track compared to the cleaned steel surface. And the $C_3H_3O_2^-/ Fe_2O_3^-$ ratio was 16.7 times higher inside the friction track compared to cleaned steel surface. Outside of the friction scar, we had 26.3 times more $CHO_2^-/Fe_2O_3^-$, 103.3 times more $C_2H_3O^-/Fe_2O_3^-$, and 15.3 times more $C_3H_3O_2^-/ Fe_2O_3^-$ compared to the cleaned steel flat.
These results show that the fragments characteristic of the PFM molecule ($C_2H_3O^-$, $C_3H_3O_2^-$, CHO_2^-) were found in much more significant amounts inside and outside the wear tracks than on the cleaned steel flat. We can therefore conclude that the organic species already existed on the cleaned steel surfaces but the major part of the signal obtained when the steel flat was in contact with the molecule came from the PFM molecule. Only slight differences were found inside and outside the wear tracks, suggesting that the PFM molecule adsorbs on steel in similar amounts both inside and outside the wear tracks in case of reciprocating test.

	$\frac{A_{CHO_2^-}}{A_{Fe_2O_3^-}}$	$\frac{A_{C_3H_3O_2^-}}{A_{Fe_2O_3^-}}$	$\frac{A_{C_2H_3O^-}}{A_{Fe_2O_3^-}}$
Flat cleaned_No friction test	0.262	0.006	0.009
Flat_Inside friction scar	7.490	0.102	1.137
Flat_Outside friction scar	6.829	0.092	0.928

Table 3: Ratios of area under curves of molecules over iron oxide for different specimens (cleaned steel flat and reciprocating tribometer flat samples).

3.4. AFM analysis

The nanoshaving experiments were performed on a sample flat obtained from a reciprocating ball-on-flat tribotest. As mentioned in § 2.4, the goal of the nanoshaving test was to show whether the additive was adsorbed on the surface of the steel flat and not to mimic the macroscopic tribotest. This measurement was carried out directly with PAO4 + 1% wt PFM at 100°C outside the friction track.
Figure 9 shows a topography image recorded after two different trials. We can distinguish two distinct square areas from the rest of the sample after the shaving tests. Outside the square area, the polishing scratches on the steel plane are still visible, as on a freshly cleaned flat sample. Between the square area and the rest of the sample, height changes are very low (around 2 nm). A reference nano-shaving experiment on pure steel with only base oil shows absolutely no damage to the surface and no changes of height are observed. The decrease in height in these shaving zones could correspond to the removal of the entire additive film or just a local reorganization of the additive film after the tip passage, for example by aligning the polymer chains parallel to the surface, which would also generate a decrease in thickness. We are not sure of any of these propositions, but what is certain is that this test confirmed that there additive was indeed adsorbed on the surface of the steel plane.

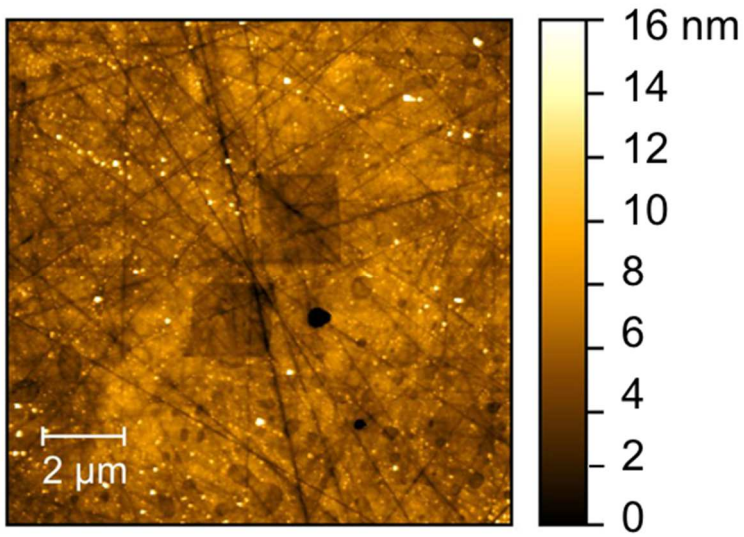

Figure 9: 10x10 mm² topography Image after 2 nanoshaving experiments performed in situ (100°C, PAO 4 + 1 % wt PFM) outside track.

3.5. DLS

DLS experiments were carried out to investigate the organization of the polymer in solution. The results showing variations of polymer size population with temperature are presented in supplementary material SM2.

4. Discussion

Mechanism of friction reduction by the PFM

For all the friction experiments (MTM and reciprocating tests), low friction ($\mu \leq 0.05$) was always achieved at 100°C even under severe lubrication conditions when usually boundary lubrication additives like MoDTC are active. This confirmed the results obtained previously [6,11] showing that polar diblock polymers could reduce friction up to 150°C even at low entrainment speeds. This was explained by the formation of a polymer adsorbed layer on the rubbing surfaces. The results obtained with the PFM studied here also suggest the presence of such adsorbed layers on the steel surfaces. For example, ECR measurements carried out during reciprocating friction tests showed the presence of an insulative layer within the contact which had an influence on friction. Then, ToF SIMS characterizations of the tribofilms provided further understanding of the organization of the molecules on the steel rubbing surfaces. Indeed, all the Tof-SIMS profiles obtained inside the wear tracks (MTM and reciprocating tests) demonstrated the presence of a significant amount of the characteristic polar fragments of the polymer molecule PFM ($C_2H_3O^-$, $C_3H_3O_2^-$ and CHO_2^-) close to the steel substrate. We can thus conclude that an adsorption film was formed on the surfaces through polar functions (ester and PEG). AFM analysis also strongly supported the presence of an adsorbed layer on the steel surface. As mentioned previously, this is in agreement with previous work suggesting that polar PFMs adsorb on the surface, thus forming a thick layer of polymer in the contact [7]. The hydrophilic part of the polymer ensured adsorption on the surface and the hydrophobic part helped to dissolve it in the lubricant [3,8,11,16].

Such viscous polymer film adsorbed on friction surfaces enables the lubricant to be entrained into the contact down to much lower speeds than would be expected from the bulk viscosity of the lubricant [11]. It can also promote slip in such contacts and thus reduce friction [26].

Importance of temperature

For all the friction experiments (MTM and reciprocating tests), low friction ($\mu \leq 0.05$) was always achieved at high temperature (100°C) and not at ambient temperature (25°C). But how does temperature affect the action mechanism of the polymer?

DLS were carried out to investigate the organization of the polymer in solution with temperature and see if this could explain the variation of friction behavior with temperature. Indeed, with the results obtained and without further investigations it was difficult to make any correlation between the variation of polymer coil size with temperature and friction behavior. Moreover, the temperature could also have an effect on the diffusion of the polymer within the solvent before its adsorption on steel. The temperature could affect the amount of molecules adsorbed on the surface. This hypothesis also requires further analytical experiments to be verified.

Why are MTM friction tests repeatable and not reciprocating tribometer tests?

From MTM and reciprocating friction tests, it was clearly shown that reciprocating tribotests led to much more dispersed friction results than MTM ones. The ToF-SIMS results have shown also that the polymer adsorbed film seems thicker inside the wear track in case of MTM compared to reciprocating tests. Why did such differences exist despite the fact that

the contact pressure, temperature, etc. were kept similar with both tribometers? Several hypotheses can be proposed.
First of all, pure sliding was encountered in the reciprocating tribotests which was not the case with MTM (SRR varied from 50% to 150%). Indeed, the reciprocating tests should have been more severe although no significant effects of SRR from 50% to 150% on the friction coefficient were found when performing tests on MTM at various SRR.
In addition, the different kinematic configurations (reciprocating versus rotating) of these two tribometers could also be considered. We can imagine that the change of direction in the case of the reciprocating test might have destabilized the polymeric adsorbed layer in the contact.
Lastly, several other parameters could have had an impact on the supply of molecules in the contact. For example, the exposure time of the samples to the lubricant during the test could explain the greater or lesser re-adsorption of polymer continuously during the test. In the case of the MTM test, the ball rolled continuously so its kinematic length was long while in the reciprocating tribometer, the ball was fixed and the kinematic length was much shorter.
All these parameters could have had an influence on the friction behavior of the steel-steel contact working under boundary lubrication and will be further investigated in the future.

5. Conclusion

This paper focused on the study of the friction behavior of a diblock PIB-PEG PFM blended in a PAO4 base oil.
Under MTM, this polymer presented a very low friction coefficient even at low entrainment speeds and a high SRR. A strong temperature effect was observed. Using a reciprocating tribometer, low friction was sometimes found even under boundary conditions; however, the repeatability was not good. A strong temperature effect was also found. The ECR results showed that an insulating film of additive was formed inside the contact when the friction was low and that this film was fragile.

Whatever the tribometer used, low friction was achieved when the molecules adsorbed on the surface through polar ester and PEG functions of the polymer (cf ToF-SIMS, ECR measurements and AFM analysis).

Several assumptions were proposed to explain the difference between the MTM and reciprocating test results: the effect of pure rolling versus slide-to roll ratio, the effect of kinematics (reciprocating versus rotating) and the effect of contact feed.

Acknowledgements

The author would like to thank Laurent Dupuy from Science et Surfaces for performing the ToF-SIMS experiments. We would also like to thank the NanoBio-ICMG platforms (FR 2607) for access to the AFM.

References

[1] Holmberg K. Global energy consumption due to friction and wear in the mining industry. Tribol Int 2017:24.

[2] Wong VW, Tung SC. Overview of automotive engine friction and reduction trends–Effects of surface, material, and lubricant-additive technologies. Friction 2016;4:1–28.

[3] Spikes H. Friction Modifier Additives. Tribol Lett 2015;60:5.

[4] Hobday I, Eastwood J. Friction Modifiers for Next Generation Engine Oils. Lube Mag 2014:27–34.

[5] Lee S, Müller M, Ratoi-Salagean M, Vörös J, Pasche S, De Paul SM, et al. Boundary Lubrication of Oxide Surfaces by Poly(L-lysine)-g-poly(ethylene glycol) (PLL-g-PEG) in Aqueous Media. Tribol Lett 2013;15:231–9.

[6] Smeeth M, Spikes HA, Gunsel S. Boundary Film Formation by Viscosity Index Improvers. Tribol Trans 1996;39.

[7] Cusseau P, Vergne P, Martinie L, Philippon D, Devaux N, Briand F. Film Forming Capability of Polymer-Base Oil Lubricants in Elastohydrodynamic and Very Thin Film Regimes. Tribol Lett 2019;67:45.

[8] Gunsel S, Smeeth M, Spikes H. Friction and Wear Reduction by Boundary Film-Forming Viscosity Index Improvers. Warrendale, PA: SAE International; 1996.

[9] Müller M, Fan J, Spikes H. Design of Functionalized PAMA Viscosity Modifiers to Reduce Friction and Wear in Lubricating Oils. J ASTM Int 2007;4:1–10.

[10] Bielecki RM, Benetti EM, Kumar D, Spencer ND. Lubrication with Oil-Compatible Polymer Brushes. Tribol Lett 2012;45:477–87.

[11] Fan J, Müller M, Stöhr T, Spikes HA. Reduction of Friction by Functionalised Viscosity Index Improvers. Tribol Lett 2007;28:287–98.

[12] Mitsui H, Spikes HA, Suita Y. Boundary Film Formation by Low Molecular Weight Polymers. Tribol. Ser., vol. 32, 1997, p. 487–500.

[13] Tohyama M, Ohmori T, Murase A, Masuko M. Friction reducing effect of multiply adsorptive organic polymer. Tribol Int 2009;42:926–33.

[14] Van Ravensteijn BGP, Bou Zerdan R, Seo D, Cadirov N, Watanabe T, Gerbec JA, et al. Triple Function Lubricant Additives Based on Organic–Inorganic Hybrid Star Polymers: Friction Reduction, Wear Protection, and Viscosity Modification. ACS Appl Mater Interfaces 2019;11:1363–75.

[15] Thompson L, Grange T, Randles SJ, Boyde S, Gamwell J. Friction Reducing Additive. US 9.228,152 B2, 2016.

[16] Guegan J, Southby M, Spikes H. Friction Modifier Additives, Synergies and Antagonisms. Tribol Lett 2019;67:83.

[17] Hirayama T, Kawamura R, Fujino K, Matsuoka T, Komiya H, Onishi H. Cross-Sectional Imaging of Boundary Lubrication Layer Formed by Fatty Acid by Means of Frequency-Modulation Atomic Force Microscopy. Langmuir 2017;33:10492–500.

[18] Koshima H, Iyotani Y, Peng Q, Ye S. Study of Friction-Reduction Properties of Fatty Acids and Adsorption Structures of their Langmuir–Blodgett Monolayers using Sum-Frequency Generation Spectroscopy and Atomic Force Microscopy. Tribol Lett 2016;64:34.

[19] Massoud T, De Matos RP, Le Mogne T, Belin M, Cobian M, Thiébaut B, et al. Effect of ZDDP on lubrication mechanisms of linear fatty amines under boundary lubrication conditions. Tribol Int 2020;141:105954.

[20] Mazuyer D, Cayer-Barrioz J, Tonck A, Jarnias F. Friction Dynamics of Confined Weakly Adhering Boundary Layers. Langmuir 2008;24:3857–66.

[21] Lundgren SM, Persson K, Kronberg B, Claesson PM. Adsorption of fatty acids from alkane solution studied with quartz crystal microbalance. Tribol Lett 2006;22:15–20.
[22] Fry BM, Moody G, Spikes HA, Wong JSS. Adsorption of Organic Friction Modifier Additives. Langmuir 2020;36:1147–55.
[23] Lu R, Mori S, Tani H, Tagawa N, Koganezawa S. Low friction properties of associated carboxylic acids induced by molecular orientation. Tribol Int 2017;113:36–42.
[24] Kus M, Kalin M. Additive chemical structure and its effect on the wetting behaviour of oil at 100 °C. Appl Surf Sci 2020;506:145020.
[25] Spikes HA. Film-forming additives - direct and indirect ways to reduce friction. Lubr Sci 2002;14:147–67.
[26] Choo J-H, Forrest AK, Spikes HA. Influence of Organic Friction Modifier on Liquid Slip: A New Mechanism of Organic Friction Modifier Action. Tribol Lett 2007;2:239–44.